Impact of type of crystal defects in multicrystalline Si on electrical properties and interaction with impurities

Isao Takahashi,[1,a)] Noritaka Usami,[1,b)] Hiroshi Mizuseki,[1] Yoshiyuki Kawazoe,[1] Gaute Stokkan,[2] and Kazuo Nakajima[3]
[1]*Institute for Materials Research (IMR), Tohoku University, 2-1-1 Katahira, Aoba-ku, Sendai 980-8577, Japan*
[2]*Norwegian University of Science and Technology, Alfred Getz vei 2, N-7491 Trondheim, Norway*
[3]*Graduate School of Energy Science, Kyoto University, Yoshida-Honmachi, Sakyo-ku, Kyoto 606–8501, Japan*

(Received 25 September 2010; accepted 6 December 2010; published online 2 February 2011)

We investigated impact of type of crystal defects in multicrystalline Si (mc-Si) on electrical properties and their change after gettering process of impurities. A bundle of dislocations gives negative impact on the gettering process, while Σ3 grain boundaries does not affect at all. In addition, we categorized random grain boundaries in mc-Si by the contact angle between adjacent dendrite crystals to form the grain boundary. Change in the contrast of photoluminescence intensity around the grain boundary was found to systematically vary by the contact angle, which showed good correlation with calculated interface energy of the grain boundary. Grain boundaries with low interface energy are concluded to be preferable to weaken recombination activity by the gettering process and improvement of solar cell performance based on mc-Si. © *2011 American Institute of Physics*. [doi:10.1063/1.3544208]

I. INTRODUCTION

Crystal defects in multicrystalline material such as grain boundaries and dislocations are known to affect macroscopic properties of the crystal, and artificial engineering of crystal defects is regarded as one of the promising routes to control macroscopic properties of multicrystalline material.[1] Generally, local properties of crystal defects are not unique, and strongly depend on the type of crystal defects. Therefore, fundamental understanding of impact of various crystal defects on properties is of crucial importance when one intends to improve macroscopic properties by microscopic control of crystal defects.

Among various multicrystalline materials, multicrystalline Si (mc-Si) is important from viewpoints of applications as well as materials science. mc-Si is the most major starting material for solar cells among various types of solar cells, and improvement of electrical properties by controlling crystal defects is being pursued.[2–11] In addition, scientific research to disclose electrical properties of crystal defects is intensively underway. Chen *et al.*[12–14] investigated electrical properties of grain boundaries in mc-Si by electron beam induced current method, and found that electrical activity and interaction with intentionally doped iron impurities is strongly dependent on the type of grain boundaries such as low Σ, high Σ, random, and small angle grain boundaries. Kutsukake *et al.*[15] quantitatively estimated average recombination velocity of small angle boundaries, and revealed that they act as serious defects to decrease photocurrents especially when decorated with impurities. As illustrated by these examples, electrical properties of mc-Si are affected by characters of grain boundaries as well as their interaction with impurities. However, influence of grain boundary characters on electrical properties is not fully understood since grain boundaries in mc-Si are generally complicated and systematic investigation has been difficult.

Recently, we have shown that systematic variation in grain boundary characters is possible by employing faceted dendrite crystals.[16] Faceted dendrite crystals are grown from a Si melt when the amount of supercooling is larger than 10 K.[17] The faceted dendrite crystal contains a pair of (111) Σ3 boundaries in the center of the primary arm, and its upper plane can be limited to only two orientations of either {110} or {112}.[18] Therefore, if we start crystal growth of mc-Si with dendritic nucleation, grain boundaries are formed by the contact of adjacent dendrite crystals at the initial stage, and the character of grain boundaries can be systematically changed by the contact angle of adjacent dendrite crystals and their upper planes. This idea for systematic variation in the grain boundary character was utilized to confirm theoretical prediction of reduction in defect density in mc-Si by controlling grain boundaries so that shear stress around the grain boundary can be reduced.[16,19] Furthermore, control of coherency of grain boundaries would be possible if we can control the contact angle of dendrite crystals.

In this study, we investigated impact of type of crystal defects in mc-Si on electrical properties and their change after phosphorus diffusion to getter impurities. As our original approach, we utilized mc-Si with systematically changed grain boundaries by taking advantage of faceted dendrite crystals. In addition to conventional classification of crystal defects to dislocations, Σ3 boundaries, and random boundaries, we categorized random grain boundaries by the contact angle of adjacent dendrite crystals. As a consequence, we revealed that change in the electrical properties after the get-

[a)]Present address: SANYO Electric Co., Ltd., 7–3–2, Ibukidai-higashimachi, Nishi-ku, Kobe, Hyogo 651–2242, Japan.
[b)]Electronic mail: usa@imr.tohoku.ac.jp.

tering process systematically varies with the contact angle as revealed by the contrast of photoluminescence (PL) intensity around the grain boundary, and the PL contrast became almost absent when the contact angle is close to zero or satisfies the relationship to form Σ3. The tendency was found to be in good agreement with the variation in interface energy.

II. EXPERIMENTS

Mc-Si ingots used in this study were grown by directional solidification of a Si melt in a quartz crucible. The raw materials were 11*N* purity polycrystalline Si and B-doped single crystalline Si. The resistivity of the mc-Si ingots was controlled to be 1 Ω cm. The crystal growth was started with dendritic nucleation followed by solidification in a temperature gradient at a constant cooling rate of 0.5 °C/min. The diameter and the height of the ingot were 100 mm and 35 mm, respectively. Samples for characterizations were cut into wafers along the growth direction. We have carefully chosen the samples so that they contain crystal grains with grain boundaries associated with dendrite crystals for systematic study.

For gettering process of impurities, the samples were annealed at 870 °C for 1 h and at 700 °C for 4 h in Ar atmosphere after coating their surface by P_2O_3 solution. These annealing conditions were optimized so that most of the metal impurities such as Fe and Cu can sufficiently diffuse into the P_2O_3 layer. After annealing, the sample surfaces were chemically etched with HF and HNO_3 solution for 30 s to remove the P_2O_3 layer with high density of impurities.

Grain orientation and the character of grain boundaries were analyzed by electron backscattering diffraction (EBSD). The distribution of the etch-pit density was observed by measuring the spatial distribution of scattered light from etch-pits using a commercially available instrument (PVScan). In the measurement, a He–Ne laser was irradiated on the sample surface which was polished and etched with the Sopori solution[18] to obtain etch-pits. The intensity of scattered light from etch-pits was assumed to have a linear relation with dislocation density. Thus the etch-pit density can be estimated by the intensity of the scattered light from the etch-pits. The distribution of dislocation density was obtained by scanning the laser on the samples.

Electrical properties of the samples were investigated by PL imaging. For the measurement, the surface of the sample was chemically passivated with quinhydrone methanol solution so that effects of surface recombination can be minimized. The surface recombination velocity prepared with this solution was reported to be 4.2 cm/s,[20] which is comparable to that prepared with SiN layer.[21] Four light-emitting-diode arrays with the wavelength of 530 nm and excitation power of about 10 mW/cm^2 were used and PL from the samples was detected with a charge-coupled device camera through a filter to cut the incident light for excitation. Crystal defects to act as nonradiatve recombination centers appear dark in PL image.

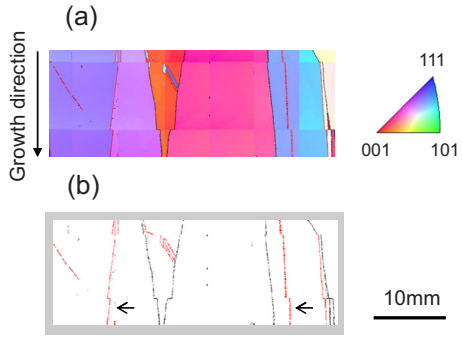

FIG. 1. (Color online) Distribution of (a) orientation and (b) grain boundary character of a typical mc-Si wafer from an ingot grown started by dendritic nucleation.

III. RESULTS

Figure 1 shows (a) orientation and (b) grain boundary distributions of a typical sample used in this study. Crystal orientation normal to the surface is represented in different colors in Fig. 1(a). Σ3 and random grain boundaries are shown in red and black lines, respectively. Discontinuity of grain boundaries in Fig. 1 is a measurement artifact caused by unintentional tilt of the sample during the EBSD measurements. Grain boundaries are seen to extend nearly parallel to the growth direction, and multicrystallne structure does not change drastically during crystal growth. Σ3 boundaries located at the center of the main arm of dendrite crystals are indicated by arrows in Fig. 1(b). Therefore, the sample consists of four large crystal grains separated by random grain boundaries.

Figure 2 shows a distribution of dislocation density in the same sample. It is seen that dislocation density is high only in a particular crystal grain, which orientation is referenced to red in Fig. 1(a). Dislocation density of the other crystal grains is found to be less than 10^4 cm^{-2}, and they can be regarded as electrically inactive.[19] We denote the region with high dislocation density as "dislocation bundle" in the following discussion.

Figure 3 shows PL images of the sample (a) before and (b) after the gettering process of impurities. After the gettering process, PL intensity in intragrain areas substantially increased since impurities are effectively removed and the minority carrier lifetime is increased. Therefore, the acquisition time of the PL image is decreased. In addition to the change in the PL intensity, PL image itself showed drastic change, depending on the type of crystal defects. Before the gettering process, dark regions can be observed in random grain boundaries and the dislocation bundle. Σ3 boundaries cannot be identified at all. The gettering process of impurities lead to various changes in the PL image. At random grain bound-

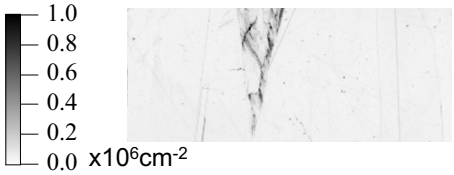

FIG. 2. Distribution of dislocation density.

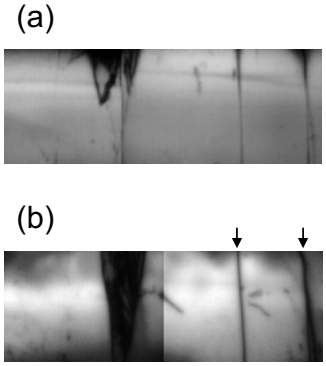

FIG. 3. Comparison of PL image of (a) before and (b) after the gettering process. Arrows indicate random grain boundaries.

aries, difference in PL intensity compared with their surroundings was enhanced. At the dislocation bundle, dark region spread toward the bottom of the sample. Σ3 boundaries were still invisible. These clearly show that the change in electrical properties depends on the type of crystal defects. In order to discuss the impact of type of crystal defects on electrical properties, we introduce PL contrast, C, defined by

$$C = \frac{I_b - I_d}{I_b}, \tag{1}$$

where I_b and I_d are the intensity in bright and dark regions, respectively. In order to quantify the contrast, line profiles across the defects were taken from the PL image. I_d was chosen as the minimum intensity at the defect and I_b was chosen as the intensity in the flat region of the line profile. This parameter, C, compensates possible inhomogeneous excitation intensity in the sample and permits us quantitative discussions.

Figure 4 shows PL contrast before and after the gettering process for (a) Σ3 grain boundaries, (b) random grain boundaries and (c) dislocation bundles. These results are summary of analysis of four samples to have experienced the same gettering process. For Σ3 grain boundaries, the PL contrast before the gettering process is quite low, and decreases

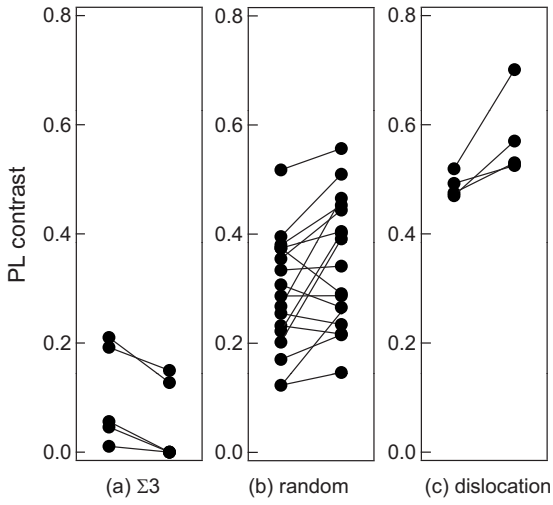

FIG. 4. PL contrast before and after the gettering process of impurities for (a) Σ3 and (b) random grain boundaries, and (c) dislocations.

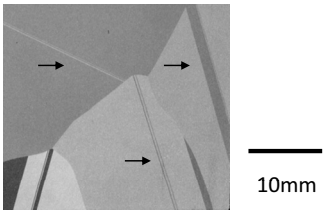

FIG. 5. Picture of the surface of a typical sample to contain large crystal grains originating from dendrite crystals. Arrows show pairs of twins at the center of the main arm of dendrite crystals.

through the gettering process. In the dislocation bundle region, the PL contrast is quite high before the gettering process and increase more after the gettering process. The PL contrast in random grain boundaries has various characteristic. Some of them behave like Σ3 grain boundaries and others are like the dislocation bundle. Besides, the change in PL contrast during the gettering process exhibit various behaviors. Some of them increase and others decrease.

In order to organize wide variety of behaviors in random grain boundary during the gettering process, random grain boundaries were categorized by the contact angle of adjacent dendrite crystals. The contact angle is defined as the angle between parallel Σ3 twin boundaries of the two dendrite crystals to form the random grain boundary. As have already mentioned, dendrite crystals have parallel twin boundaries in the center of the main arm, which indicates the growth direction. Figure 5 shows a picture of a sample cut perpendicular to the growth direction. Grain distribution can be observed by the difference in the surface reflection. The sample originates from four dendrite crystals as can be identified by parallel twins, which are located at the center of each dendrite crystal denoted by arrows. The contact angle can be easily defined using these parallel twins.

Figure 6 shows a relationship between the contact angle of dendrite crystals and PL contrast in random grain boundaries (a) before and (b) after the gettering process. Since there are two types of dendrite crystals with the upper plane of {110} and {112}, the contact of dendrite crystals has three combinations, that is {110} versus {110}, {112} versus {112}, and {110} versus {112}. In Figs. 6(a) and 6(b), no clear relationship between the contact angle and PL contrast can be recognized. Then, we attempted to calculate the difference by subtracting the PL contrast before the gettering process from that after the gettering process. Decrease in the PL contrast means that recombination at defects is suppressed. On the other hand, increase in the PL contrast indicates that crystal defects become more active for recombination. Figure 6(c) shows that the difference in PL contrast systematically decreases with decreasing the contact angle as shown in the dotted line drawn as the guide to the eye. This suggests that parallel contact of dendrite crystals is preferable to decrease recombination velocity by the gettering process. This means that the product of defect density and the capture cross section decreased. These two possibilities cannot be distinguished at this moment It should be commented that parallel contact also plays a role in suppressing generation of dislocations during growth by decreasing shear stress around

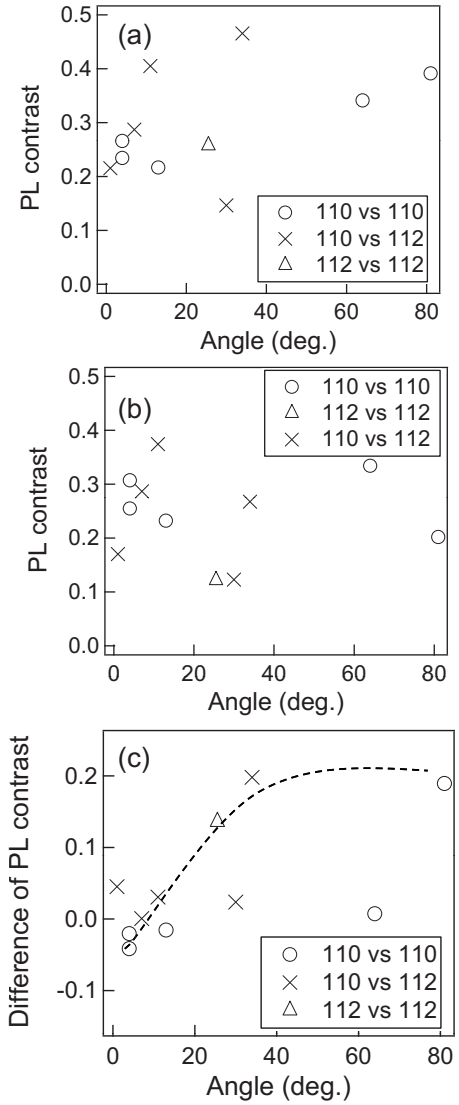

FIG. 6. Correlation between PL contrast and the contact angle of adjacent dendrite crystals (a) before and (b) after the gettering process. Difference of PL contrast before and after the gettering process is shown in (c).

the grain boundary.[16,19,22] However, contrary to this tendency, the result of the contact angle of 64° denoted by a dashed arrow does not follow the tendency.

IV. DISCUSSIONS

To explain the origin of the tendency that was seen in Fig. 6, we applied the spherical model as proposed by Lee and Choi,[23] which they employed to determine the boundary energy of pure Al. This spherical model approach has the advantage that the procedure for evaluating the misorientation dependence of the grain boundary energy can be fully computerized because one does not need to adjust the number of atoms in each single crystal to apply a two-dimensional or three-dimensional periodic boundary condition. The model generation procedure that was used in the present study is as follows. First, we prepared two spherical Si clusters from a Si crystal structure, in which the bond length and the bond angle are the values of the stable crystal structure described by Tersoff based on the empirical potential.[24] We chose the centers of the spherical clusters at random to provide various cut surfaces at the grain boundaries. We refer to the right and left clusters as two spherical clusters. Both spherical clusters are rotated independently to reproduce misorientations in the dendrite growth condition; for example, the right cluster is rotated about the [110] or the [112] orientation and the left cluster is rotated about the [110] or the [112] orientation. The [110] and [112] axes correspond to the preferred growth directions. Two axes of both clusters are fixed toward the same direction during the rotation process. Second, the right spherical cluster is rotated to the (111)-oriented surface of the left cluster, and the spherical cluster is cut in half to form a hemispherical cluster. At this point, the cut surface of the right hemispherical cluster is the (111) surface. This right hemispherical cluster is then fixed until the left cluster is prepared. Third, the left cluster is rotated to the (111)-oriented surface of the right cluster, and it is also rotated through various angles from 0° to 90°. After this procedure, this spherical cluster is also cut in half. The right and left hemispherical clusters have predetermined misorientations. These geometries correspond to a grain boundary in mc-Si under dendrite growth conditions. Finally, the two hemispherical clusters are merged and we select 1000 Si atoms from the center part to make a spherical model including a grain boundary under a given misorientation. In this case, the prepared grain boundary is located at the center of the spherical model.

To perform structural relaxation, we apply a Monte Carlo (MC) method based on the Tersoff potential[24] for the Si system by taking 100 MC steps for the hemispherical cluster as one unit, and 500 MC steps for all of the Si atoms in the spherical cluster. The displacement of each MC step is set to 0.01 Å. After the relaxation MC step, we obtain a specific grain boundary configuration of dendrite growth Si. We then evaluate the potential energy of the spherical model including all 1000 Si atoms, allowing for relaxation at the surface and at the grain boundary. The computed potential energy of the spherical sample is different from the ideal bulk energy of the crystal structure region due to the existence of the spherical free surface and the grain boundary. The free surfaces that are created in each sample have nearly the same areas, which correspond to nearly the same numbers of Si atoms. In the present study, we assume that the contributions of the free surface and of the crystal structure region are the same; namely, the energy difference in each model is only affected by the grain boundary geometry.

A spherical model for evaluating total energy has been applied to a specific grain boundary of dendrite growth Si. 600 000 different randomly-cut surface configurations were generated using the above-mentioned method, and each configuration was analyzed to evaluate the grain boundary energy as a function of the misorientations of both crystalline grains. The lowest energy of some configurations at each misorientation is selected as the total energy of each misorientation. Figure 7 shows the total energy of 1000 atoms including a grain boundary for ⟨110⟩ or ⟨112⟩ oriented mc-Si as a function of the misorientation with respect to the [111] direction, computed in the present study using the Tersoff potential. In Fig. 7(a), one relatively small cusp exists at about 72°, which corresponds to the Σ3 boundary. The ex-

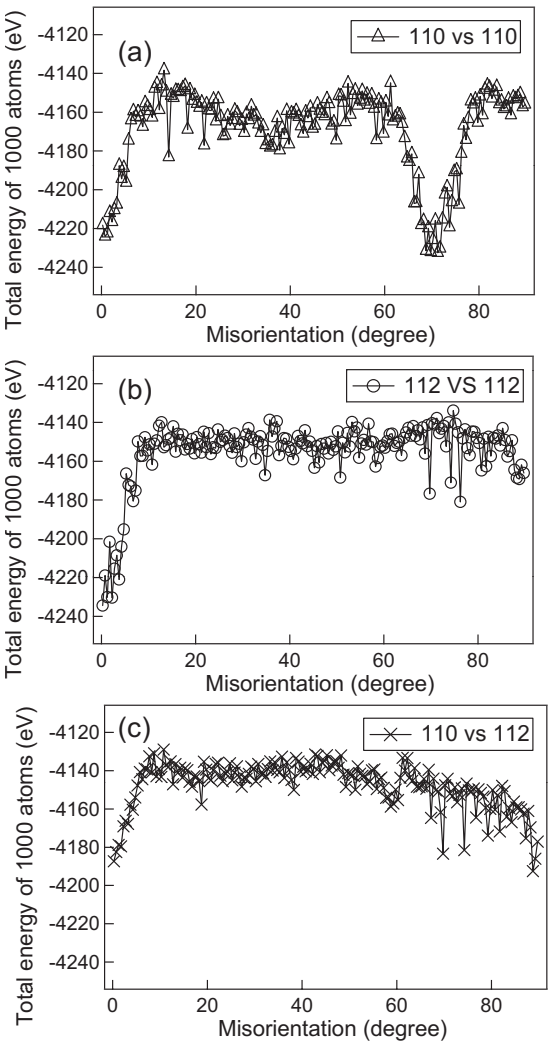

FIG. 7. Computed total energy of 1000 atoms in a spherical model as a function of misorientation with respect to the [111] direction. (a) Right orientation is [110], left orientation is [110]. (b) Right [112], left [112]. (c) Right [110], left [112].

perimental data are for finite temperature, while the present computation was performed at 0 K. Nevertheless, these values are in good agreement with the experimental results for various misorientations.

These show that grain boundaries with lower interface energy are favorable to suppress recombination activity by the gettering process. Therefore, such grain boundaries do not act as sinks for impurities, leading to efficient removal of impurities by external gettering. The dendritic nucleation at the initial stage of the crystal growth and further control of relative rotation angle of adjacent dendrite crystal is considered to be useful for controlling grain boundaries in mc-Si, which will result in efficient gettering of impurities and improvement of solar cell performance.

V. CONCLUSIONS

We attempted to investigate impact of type of crystal defects in mc-Si on electrical properties through the gettering process by using change in PL contrast. A bundle of dislocations gives negative impact on the gettering process, while $\Sigma 3$ boundaries does not affect at all. Properties of random grain boundaries are not unique, and systematically changes with the contact angle of dendrite crystals to form the grain boundary. Comparison of experiments and calculations of interface energy revealed that grain boundaries with lower interface energy are preferable to decrease recombination activity of crystal defects by the getttering process. Therefore, control of grain boundaries in mc-Si by utilizing dendritic nucleation is concluded to be useful not only for suppression of dislocations but for efficient gettering process.

ACKNOWLEDGMENTS

This works was partially supported by a Grant-in-Aid for Scientific Research (S) (20226001) from the Ministry of Education, Culture, Sports, Science, and Technology of Japan, and the New Energy and Industrial Technology Development Organization (NEDO) of Japan. One of the authors (I.T.) acknowledges the support by Global COE Program "Materials Integration (International Center of Education and Research), Tohoku University.

[1]T. Watanabe, Res. Mechanica: International Journal of Structural Mechanics and Materials Science **11**, 47 (1984).
[2]T. Buonassisi, A. A. Istratov, M. A. Marcus, B. Lai, Z. Cai, S. M. Heald, and E. R. Weber, Nature Mater. **4**, 676 (2005).
[3]K. Fujiwara, W. Pan, N. Usami, K. Sawada, M. Tokairin, Y. Nose, A. Nomura, T. Shishido, and K. Nakajima, Acta Mater. **54**, 3191 (2006).
[4]O. Schultz, S. W. Glunz, S. Riepe, and G. P. Willeke, Prog. Photovoltaics **14**, 711 (2006).
[5]M. Heuer, T. Buonassisi, M. A. Marcus, A. A. Istratov, M. D. Pickett, T. Shibata, and E. R. Weber, Phys. Rev. B **73**, 235204 (2006).
[6]M. D. Pickett and T. Buonassisi, Appl. Phys. Lett. **92**, 122103 (2008).
[7]K. Hartman, M. Bertoni, J. Serdy, and T. Buonassisi, Appl. Phys. Lett. **93**, 122108 (2008).
[8]I. Takahashi, N. Usami, R. Yokoyama, Y. Nose, K. Kutsukake, K. Fujiwara, and K. Nakajima, Jpn. J. Appl. Phys. **47**, 8790 (2008).
[9]R. Krain, S. Herlufsen, and J. Schmidt, Appl. Phys. Lett. **93**, 152108 (2008).
[10]N. Stoddard, B. Wu, I. Witting, M. Wagener, Y. K. Park, G. Rozgonyi, and R. Clark, Solid State Phenom. **131–133**, 1 (2008).
[11]Y. Nose, I. Takahashi, W. Pan, N. Usami, K. Fujiwara, and K. Nakajima, J. Cryst. Growth **311**, 228 (2009).
[12]J. Chen, T. Sekiguchi, D. Yang, F. Yin, K. Kido, and S. Tsurekawa, J. Appl. Phys. **96**, 5490 (2004).
[13]J. Chen, T. Sekiguchi, R. Xie, P. Ahmet, T. Chikyo, D. Yang, S. Ito, and F. Yin, Scr. Mater. **52**, 1211 (2005).
[14]J. Chen and T. Sekiguchi, Jpn. J. Appl. Phys., Part 1 **46**, 6489 (2007).
[15]K. Kutsukake, N. Usami, T. Ohtaniuchi, K. Fujiwara, and K. Nakajima, J. Appl. Phys. **105**, 044909 (2009).
[16]N. Usami, R. Yokoyama, I. Takahashi, K. Kutsukake, K. Fujiwara, and K. Nakajima, J. Appl. Phys. **107**, 013511 (2010).
[17]K. Fujiwara, K. Maeda, N. Usami, G. Sazaki, Y. Nose, A. Nomura, T. Shishido, and K. Nakajima, Acta Mater. **56**, 2663 (2008).
[18]K. Nagashio and K. Kuribayashi, Acta Mater. **53**, 3021 (2005).
[19]I. I. Takahashi, N. Usami, K. Kutsukake, K. Morishita, and K. Nakajima, Jpn. J. Appl. Phys. **49**, 04DP01 (2010).
[20]H. Takato, I. Sakata, and R. Shimokawa, Jpn. J. Appl. Phys., Part 2 **41**, L870 (2002).
[21]T. Lauinger, J. Schmidt, A. G. Aberle, and R. Hezel, Appl. Phys. Lett. **68**, 1232 (1996).
[22]I. Takahashi, N. Usami, K. Kutsukake, G. Stokkan, K. Morishita, and K. Nakajima, J. Cryst. Growth **312**, 897 (2010).
[23]B.-J. Lee and S.-H. Choi, Modell. Simul. Mater. Sci. Eng. **12**, 621 (2004).
[24]J. Tersoff, Phys. Rev. B **39**, 5566 (1989).